HHS Public Access

Author manuscript

Nat Commun. Author manuscript; available in PMC 2013 October 21.

Published in final edited form as:

Nat Commun. 2013 ; 4: 2598. doi:10.1038/ncomms3598.

Smurf2 suppresses B-cell proliferation and lymphomagenesis by mediating ubiquitination and degradation of YY1

Charusheila Ramkumar[1], **Hang Cui**[1], **Yahui Kong**[1], **Stephen N. Jones**[1], **Rachel M. Gerstein**[2], and **Hong Zhang**[1,*]

[1]Department of Cell and Developmental Biology, University of Massachusetts Medical School, Worcester, MA 01655, USA

[2]Department of Microbiology and Physiological Systems, University of Massachusetts Medical School, Worcester, MA 01655, USA

Abstract

About half of patients with diffuse large B-cell lymphoma (DLBCL) do not respond to or relapse soon after the standard chemotherapy, indicating a critical need to better understand the specific pathways perturbed in DLBCL for developing effective therapeutic approaches. Mice deficient in the E3 ubiquitin ligase Smurf2 spontaneously develop B-cell lymphomas that resemble human DLBCL with molecular features of germinal center or post-germinal center B cells. Here we show that Smurf2 mediates ubiquitination and degradation of YY1, a key germinal center transcription factor. Smurf2 deficiency enhances YY1-mediated transactivation of *c-Myc* and B-cell proliferation. Furthermore, Smurf2 expression is significantly decreased in primary human DLBCL samples, and low levels of Smurf2 expression correlate with inferior survival in DLBCL patients. The Smurf2-YY1-c-Myc regulatory axis represents a novel pathway perturbed in DLBCL that suppresses B-cell proliferation and lymphomagenesis, suggesting pharmaceutical targeting of Smurf2 as a new therapeutic paradigm for DLBCL.

Introduction

In response to antigen stimulation, B cells undergo extensive proliferation to form germinal centers (GCs) in secondary lymphoid organs[1]. As a consequence of cell proliferation, mutagenic events may occur and target cancer-causing genes. In addition, B cells in GCs undergo distinct genetic processes to generate high-affinity antibodies, including somatic hypermutation (SHM) of the variable region of the immunoglobulin gene and class switch

*To whom correspondence should be addressed: Hong Zhang, Department of Cell and Developmental Biology, University of Massachusetts Medical School, 55 Lake Avenue North, Worcester, MA 01655, USA. Phone: 508-856-5423; Fax: 508-856-1033; hong.zhang@umassmed.edu.

Conflict of Interest

The authors declare no competing financial interest.

Author Contributions

C.R, R.M.G and H.Z. developed the concept and designed the experiments; C.R., H.C., Y.K., R.M.G and H.Z. did the experiments and/or analyzed data; S.N.J. contributed reagents, intellectual input and editorial assistance; C.R. and H.Z. wrote the paper; H.Z. supervised the project and obtained funding.

recombination (CSR) that changes immunoglobulin class. These processes can target non-immunoglobulin genes in the GC B cells, leading to genetic alterations that promote tumorigenesis[2, 3, 4, 5, 6, 7, 8]. To counteract these oncogenic effects, it has been postulated that tumor suppressors function to constrain the proliferation and survival of GC B cells at risk of malignant transformation. Identification of these specific tumor suppressors is critical to our understanding of malignancies originated in GCs.

Most non-Hodgkin's lymphomas (NHLs) are derived from GC B cells or B cells that have passed through GCs[9, 10]. Diffuse large B-cell lymphoma (DLBCL) is the most common type of NHL, accounting for 30–40% of all new diagnoses[11]. Significant progress has been made in our understanding of the dysregulated pathways and genetic abnormalities that govern the development of DLBCL[10, 12, 13]. Current chemotherapy regimens using the combination of cyclophosphamide, doxorubicin, vincristine, and prednisone (CHOP), together with the anti-CD20 monoclonal antibody rituximab (R-CHOP), result in long-term remission in approximately 50% of DLBCL patients[14]. However, a significant fraction of DLBCL are still incurable, indicating that further understanding of the pathogenesis of this disease is needed in order to develop specific and effective therapeutic approaches.

Recently it has been shown that mice deficient in Smurf2 (Smad ubiquitination regulatory factor-2) spontaneously develop tumors including lymphomas of B-cell origin, indicating that Smurf2 functions as a tumor suppressor[15, 16]. It has been proposed that Smurf2 exerts its tumor suppressor function through its ability to maintain genomic integrity[15] and regulate senescence[16]. In this report, we find that B-cell lymphomas developed in Smurf2-deficient mice resemble human DLBCL with molecular features of GC or post-GC B cells. We discover that Smurf2 ubiquitinates YY1, a master regulator of GC transcriptional program[17], through which Smurf2 suppresses cell proliferation and *c-Myc* expression. This Smurf2-YY1-cMyc regulatory axis provides novel insight into lymphomagenesis in GC or post-GC B cells and is highly relevant in human DLBCL.

Results

B-cell lymphoma in Smurf2-deficient mice resembles DLBCL

Previously we have shown that Smurf2-deficient (*Smurf2*$^{T/T}$, T for the gene-trapped *Smurf2* allele) or the heterozygous *Smurf2*$^{+/T}$ mice exhibit increased susceptibility to spontaneous tumorigenesis after 12 months of age, with the majority of tumors (72.7%) being lymphomas in spleen with a B-cell origin (i.e., B220^{+}). All tumor-bearing *Smurf2*$^{T/T}$ or *Smurf2*$^{+/T}$ mice have enlarged spleens[16], prompting us to characterize spleens in mice before malignancy. Compared with wild-type mice, an increase in spleen weight relative to body weight was found in 2-month old *Smurf2*$^{T/T}$ mice (Fig. 1a; 45.2% increase, P=0.021, Student t-test) or *Smurf2*$^{+/T}$ mice (Supplementary Fig. S1a; 22.5% increase, P=0.07, Student t-test). This increase in spleen weight was accompanied by an increase in total splenic cells (Fig. 1b) and B220^{+} B cells (Fig. 1c), meanwhile the frequency of splenic B220^{+} B cells remained unchanged in young *Smurf2*$^{T/T}$ compared to wild-type mice (Fig. 1c). Further, we analyzed B-cell development in bone marrow and spleen using flow cytometry. Between young *Smurf2*$^{T/T}$ and wild-type mice, we found no obvious difference in the frequencies of various B-cell sub-populations in bone marrow (Supplementary Fig. S2 and S3) and spleen

(Fig. 1d, Fig. 2 and Supplementary Fig. S4), suggesting that B-cell development and differentiation are normal in Smurf2-deficient mice.

In lymphoma-bearing spleens of Smurf2-deficient mice, we observed a significant expansion (average 6.3-fold increase compared to wild-type mice) of $IgD^{neg}IgM^{low}$ B cells that were CD23 negative and heterogeneous for CD24 (Fig. 3a), suggesting a GC or post-GC phenotype. This expansion of $IgD^{neg}IgM^{low}$ B cells in tumor-bearing mice is in sharp contrast with young mice before malignancy, in which the frequency of the $IgD^{neg}IgM^{low}$ B-cell population was similar between young Smurf2-deficient and wild-type mice (Fig. 1d). Consistent with being GC-derived, these lymphomas showed positive staining for the GC markers peanut agglutinin (PNA) and CD95 (Fig. 3b,c), underwent class switch recombination to immunoglobulin γ2a (Fig. 3c and Supplementary Fig. S5) and exhibited increased somatic hypermutation in the immunoglobulin heavy chain (*IgH*) locus (Supplementary Table S1). Moreover, these lymphomas showed a gene expression pattern analogous to that in human DLBCL (Supplementary Fig. S6a). Collectively, these data indicate that lymphomas developed in Smurf2-deficient mice are GC or post-GC derived and have molecular features consistent with DLBCL[18].

We analyzed the genomic rearrangements of the *IgH* locus in representative lymphoma-bearing spleen samples, and detected a specific V(D)J rearrangement in some lymphoma samples (Supplementary Fig. S6b), consistent with a clonal origin of these lymphomas. The lack of detection of a rearrangement using the largest V_H family (J588) in other lymphoma samples may reflect the presence of non-neoplastic cells in spleen samples, rearrangement with a different V_H family, or oligoclonal origin. To further investigate tumorigenicity of Smurf2-deficient lymphomas, we injected splenic cells from lymphoma-bearing Smurf2-deficient mice into sub-lethally irradiated *Rag1* knockout (*Rag1*$^{-/-}$) mice. *Rag1*$^{-/-}$ recipient mice became moribund 6–8 weeks after injection. An extensive expansion of $IgD^{neg}IgM^{low}$ B cells was observed in the spleens of these *Rag1*$^{-/-}$ recipients (Fig. 3c). While injected splenic cells contained 1.2–1.3×10^5 $IgD^{neg}IgM^{low}$ B cells, 1.7–8.2×10^6 $IgD^{neg}IgM^{low}$ B cells were recovered in *Rag1*$^{-/-}$ mice, representing a 13 to 67-fold increase of this population. Furthermore, these $IgD^{neg}IgM^{low}$ B cells stained positively for CD95, consistent with a GC-derived phenotype (Fig. 3c). Positive staining for IgG2a confirmed that these tumors underwent class switch recombination (Fig. 3c). Given that the expanded population of $IgD^{neg}IgM^{low}$ B cells in *Rag1*$^{-/-}$ mice had the same GC B-cell phenotype as the injected tumor cells, and that the recipient *Rag1*$^{-/-}$ mice became moribund, these data are consistent with transfer of disease resembling DLBCL.

Enhanced proliferation in Smurf2-deficient splenic B cells

Lymphomas found in Smurf2-deficient mice showed an increase in the frequency of cells positive for the cell proliferation-associated antigen Ki-67 compared to spleen sections of age-matched wild-type mice (Fig. 4a). Interestingly, Ki-67 staining was increased in spleen, particularly white pulp, of 2-month old *Smurf2*$^{T/T}$ (Fig. 4b, c) or *Smurf2*$^{+/T}$ mice (Supplementary Fig. S1b) compared to wild-type littermates. Furthermore, increased bromodeoxyuridine (BrdU) incorporation was detected in $B220^+$ splenic B cells (Fig. 4d) or total splenic cells (Supplementary Fig. S7a) of young *Smurf2*$^{T/T}$ mice compared to wild-type

littermates. Taken together, these results suggest that increased cell proliferation observed in Smurf2-deficient splenic B cells and B-cell lymphomas is caused by reduced Smurf2 expression rather than as a consequence of tumorigenesis.

To further analyze cell proliferation in splenic B cells, we cultured total spleen cells of 2-month old wild-type or *Smurf2*$^{T/T}$ mice with the B-cell mitogen lipopolysaccharide (LPS). In response to LPS, *Smurf2*$^{T/T}$ splenic B220^{+} B cells proliferated significantly better than wild-type cells (Fig. 4e), whereas cell viability was similar between them (Supplementary Fig. S7b). Using carboxyfluorescein succinimidyl ester (CFSE) to track cell divisions in cultured splenic B cells, we found that the number of *Smurf2*$^{T/T}$ splenic B cells undergoing successive cell divisions was significantly increased compared to wild-type cells (Fig. 4f and Supplementary Fig. S7c). Without LPS stimulation, cell death was similar between wild-type and *Smurf2*$^{T/T}$ B cells (Fig. 4e and Supplementary Fig. S7b). Furthermore, TUNEL staining for apoptosis was similar when spleen sections from 2-month old *Smurf2*$^{T/T}$ mice or lymphomas were compared to age-matched wild-type mice (Fig. 4a, b). Both observations suggest that apoptosis is unchanged in Smurf2-deficient cells. Collectively, these results indicate that cell proliferation is enhanced in *Smurf2*$^{T/T}$ splenic B cells, suggesting a possible mechanism underlying increased B-cell lymphomagenesis in Smurf2-deficient mice.

Elevated c-Myc expression in Smurf2-deficient mice

As up-regulation of c-Myc is frequently observed in B-cell lymphoma, and forced expression of c-Myc drives lymphomagenesis in mice[19, 20, 21], it prompted us to examine c-Myc expression in lymphomas derived from *Smurf2*$^{T/T}$ or *Smurf2*$^{+/T}$ mice. The expression of *c-Myc* mRNA in these lymphomas was increased compared with spleens of wild-type mice of the similar age (Fig. 5a), while no *IgH-Myc* translocation was detected in lymphomas in Smurf2-deficient mice (Supplementary Fig. S8).

To understand whether c-Myc elevation underlies increased B-cell proliferation and lymphomagenesis in Smurf2-deficient mice, we examined c-Myc expression in young *Smurf2*$^{T/T}$ mice at the pre-neoplastic stage. We found an increase in c-Myc expression in spleen (Fig. 5b) and liver (Supplementary Fig. S9a, b) of 2-month old *Smurf2*$^{T/T}$ mice compared with age-matched wild-type mice, suggesting that Smurf2 deficiency leads to increased c-Myc expression. To further corroborate *c-Myc* mRNA elevation with Smurf2 deficiency, we examined the transcript levels of c-Myc transactivation targets *Apex1*, *Cad* and *Ncl*, which have been validated as c-Myc targets in multiple studies, but are not directly involved in cell proliferation (http://www.myccancergene.org/site/mycTargetDB.asp)[22]. We found increased transcript levels of these c-Myc targets in lymphomas (Fig. 5c) as well as spleen (Fig. 5d) and liver of young *Smurf2*$^{T/T}$ mice (Supplementary Fig. S9c).

Smurf2 ubiquitinates YY1 to regulate *c-Myc* expression

To investigate the underlying mechanism of Smurf2-mediated regulation of c-Myc expression, we searched for transcriptional regulators that have been shown to transactivate *c-Myc* and examined their potential as the ubiquitination targets of Smurf2. We reasoned that stabilization of such a transcriptional regulator in Smurf2-deficient mice could be responsible for elevated expression of *c-Myc*. YY1, which transactivates *c-Myc*[23, 24] and is a

central regulator of the GC B-cell-specific transcriptional program[17], contains a PPDY motif that can potentially interact with the WW domains in Smurf2. We found that the protein levels of YY1 were increased in lymphomas derived from *Smurf2*$^{T/T}$ or *Smurf2*$^{+/T}$ mice (Fig. 6a) as well as in spleen (Fig. 6b) and liver (Supplementary Fig. S9b) of young *Smurf2*$^{T/T}$ mice compared with wild-type littermates. In contrast, the transcript level of *YY1* was largely unchanged in Smurf2-deficient mice (Fig. 6b), suggesting a post-transcriptional regulation of YY1 by Smurf2. Supporting this notion, the protein half-life of YY1 was increased from 2.1-hr in wild-type splenic B cells to 4.4-hr in splenic B cells of *Smurf2*$^{T/T}$ mice (Fig. 6c), suggesting that Smurf2 deficiency leads to an increase in protein stability of YY1.

To further characterize Smurf2-mediated regulation of YY1, we stably expressed short-hairpin RNA (shRNA) targeting *Smurf2* in a human DLBCL cell line (SUDHL-6), and found that down-regulation of *Smurf2* led to an increase in YY1 protein (Fig. 7a). Conversely, ectopic expression of Smurf2 resulted in a reduction in the steady-state level of YY1 protein. In contrast, a ligase mutant C716A, in which the conserved cysteine at residue 716 is replaced by alanine to abolish its E3 ubiquitin ligase activity[25, 26, 27], did not lead to changes in YY1 (Fig. 7b), indicating that regulation of YY1 bySmurf2 requires its ubiquitin ligase activity. Consistent with what we found in Smurf2-deficient mice (Fig. 5), *c-Myc* transcripts were regulated by Smurf2 (Fig. 7a, b). In contrast, *YY1* transcripts were largely unchanged when Smurf2 expression was altered (Fig. 7a, b), consistent with the notion that Smurf2 regulates YY1 post-transcriptionally. These results led us to hypothesize that Smurf2 is the E3 ubiquitin ligase responsible for ubiquitination of YY1.

To test this hypothesis, we first investigated whether Smurf2 interacts with YY1, as the C2-WW-HECT class of E3 ligases interacts with their protein substrates to catalyze ubiquitination. To limit potential degradation of YY1 by Smurf2, we used the ligase mutant C716A in co-immunoprecipitation with YY1. Smurf2 and YY1 were found to form a complex by co-immunoprecipitation, whereas deletion of the PPDY motif of YY1 (ΔPY) abolished the Smurf2-YY1 interaction (Fig. 7c). Furthermore, we found that three WW domains (i.e. WWs), but not the C2 or HECT domain of Smurf2 alone, were sufficient to interact with YY1. Deletion of the N-terminal WW domain (ΔWW1) abolished the interaction between Smurf2 and YY1 (Fig. 7c). Collectively, these results indicate that the Smurf2-YY1 interaction is mediated by the WW domains of Smurf2 and the PPDY motif of YY1.

We next investigated whether Smurf2 induces ubiquitination of YY1. Ubiquitination of YY1 was greatly induced in the presence of Smurf2 compared with a GFP control, whereas catalytically inactive C716A lost the ability to ubiquitinate YY1 (Fig. 7d and Supplementary Fig. S10). Furthermore, deletion of the PPDY motif in YY1 diminished Smurf2-mediated ubiquitination (Fig. 7d and Supplementary Fig. S10). Conversely, we used stably expressed shRNA to knockdown the expression of Smurf2 in SUDHL-6 cells, and found that down-regulation of Smurf2 resulted in decreased ubiquitination of endogenous YY1 (Fig. 7e). Collectively, these results indicate that Smurf2 is the E3 ubiquitin ligase responsible for ubiquitination of YY1.

YY1 has been shown to bind to the human *c-Myc* promoter in a chromatin immunoprecipitation (ChIP) assay and to be sufficient to up-regulate *c-Myc* expression[23, 24]. We expressed shRNA to knockdown *YY1* expression in SUDHL-6 cells, and found that *c-Myc* transcripts were decreased upon *YY1* down-regulation (Fig. 8a), indicating that YY1 is required to regulate c-Myc expression. As shRNA knockdown of *Smurf2* expression in SUDHL-6 cells led to elevation of c-Myc, further down-regulation of *YY1* by shRNA resulted in decreased c-Myc expression (Fig. 8b), suggesting that YY1 is the critical mediator of Smurf2-regulated c-Myc expression. Further supporting this notion, knockdown of YY1 expression by siRNA led to down-regulation of c-Myc in primary B cells isolated from spleens of wild-type and *Smurf2*$^{T/T}$ mice (Fig. 8c). Moreover, ChIP analysis indicated that YY1 was bound to the *c-Myc* promoter in mouse spleen, and this binding was increased in spleen of *Smurf2*$^{T/T}$ mice compared with wild-type mice (Fig. 8d), consistent with the mechanism in which stabilization of YY1 in Smurf2-deficient cells up-regulates c-Myc expression.

Smurf2 and YY1 regulate proliferation of DLBCL cells

To understand the consequence of Smurf2-mediated ubiquitination of YY1 in lymphomagenesis, we investigated the Smurf2-YY1 axis in regulation of cell proliferation in human DLBCL cells. Consistent with our observation of increased cell proliferation in Smurf2-deficient mice, shRNA knockdown of *Smurf2* expression inSUDHL-6 cells (Fig. 8b) led to enhanced cell proliferation (Fig. 8e). Down-regulation of *YY1* by shRNA (Fig. 8b) resulted in decreased proliferation in SUDHL-6 cells, indicating that YY1 is a critical regulator of cell proliferation in DLBCL cells (Fig. 8e). Furthermore, down-regulation of *YY1* in SUDHL-6 cells that already had shRNA knockdown of *Smurf2* (Fig. 8b) alleviated the increase in cell proliferation mediated by Smurf2 deficiency (Fig. 8e), suggesting that Smurf2 regulates cell proliferation through YY1. Conversely, ectopic expression of wild-type Smurf2, but not the ligase mutant C716A, in SUDHL-6 cells (Fig. 7b) led to significantly decreased cell proliferation (Fig. 8f), while apoptosis was not significantly changed (Fig. 8g). Taken together, these results indicate the Smurf2-YY1 regulatory axis is critical in proliferation of lymphoma cells, providing a plausible mechanism underlying increased cell proliferation and lymphomagenesis in Smurf2-deficient mice.

Smurf2 expression correlates with DLBCL patient survival

To investigate whether Smurf2 deficiency has clinical relevance in human lymphomagenesis, we analyzed Smurf2 expression in primary human lymphoma samples. In a published microarray dataset (GSE2350) that contains samples of human primary B-cell lymphoma and normal B cells[28], we found that the expression of Smurf2 was significantly decreased in DLBCL, Burkitt's lymphoma and follicular lymphoma compared to normal B cells (Fig. 9a).

To further understand the relevance of decreased Smurf2 expression in human lymphomagenesis, we next investigated whether the level of Smurf2 expression correlates with clinical outcome. Smurf2 expression has been measured in three human primary B-cell lymphoma microarray datasets, each of which contains survival information of more than 100 patients[29, 30, 31]. Within each dataset, we divided lymphoma samples into four groups

based on the level of Smurf2 expression, with the 1st quartile having the lowest Smurf2 expression. Survival analysis of dataset GSE4475 in Gene Expression Omnibus (GEO, http://www.ncbi.nil.nih.gov/geo), which contains DLBCL and some Burkitt's lymphoma patients[29], showed that overall survival of patients with the lowest Smurf2 expression (1st quartile) was significantly worse ($P<0.0001$, log-rank test) than that of patients with higher Smurf2 expression (2nd–4th quartile) (Fig. 9b). Similarly, a significantly poor survival prognosis ($P=0.0004$, log-rank test) was observed in patients with low level of Smurf2 expression (1st and 2nd quartiles) compared to patients with high level of Smurf2 expression (3rd and 4th quartiles) in an independent dataset GSE10846 in GEO (Fig. 9c), which contains only DLBCL patients[30]. Interestingly, we found no significant difference in overall survival of patients in a human follicular lymphoma dataset[31] based on Smurf2 expression level (Fig. 9d), suggesting a specific role of Smurf2 deficiency in human DLBCL or possibly Burkitt's lymphoma.

Certain clinical and molecular parameters have been shown to predict DLBCL patient survival[32, 33, 34]. Univariate analysis indicated a significant correlation between poor survival prognosis and age, Ann Arbor stage, molecular subtype, or International Prognostic Index (IPI) score. To determine whether Smurf2 expression can predict clinical outcomes independently of these known parameters, we carried out a multivariate Cox regression analysis, and found that low level of Smurf2 expression was an independent predictor of patient survival in both DLBCL cohorts ($P=0.01$ for GSE4475 and $P=0.027$ for GSE10846) (Table 1). These results indicate that Smurf2 expression is a valuable prognostic marker for DLBCL patient survival, and further suggest that Smurf2 is a potential therapeutic target for DLBCL.

Discussion

In this study, we found that lymphomas developed in Smurf2-deficient mice have molecular features of GC or post-GC B cells and resemble human DLBCL. A significant decrease in Smurf2 expression is found in human DLBCL compared to normal B cells, indicating the clinical relevance of Smurf2 deficiency in human lymphomagenesis. Furthermore, our finding that low levels of Smurf2 expression correlate with poor survival prognosis in DLBCL patients suggests that Smurf2 is part of an important molecular pathway controlling lymphoma development. This pathway, identified in this study as the Smurf2-YY1-c-Myc regulatory axis, is novel and specific in suppression of B-cell proliferation and consequently lymphomagenesis. To our knowledge, Smurf2 is the first E3 ligase identified to ubiquitinate YY1. As a transcriptional regulator, YY1 plays a critical role in many biological processes including development, differentiation and proliferation, and has been implicated in oncogenesis[35, 36]. Specific to B cells, YY1 is a critical regulator of B-cell development[37], and has recently been identified as a central regulator of the GC B-cell-specific transcriptional program[17]. The expression of YY1 is found to be increased in high-grade DLBCL or Burkitt's lymphoma compared to low grade lymphoma or normal B cells[38]. Furthermore, elevated YY1 expression correlates with poor survival prognosis of DLBCL patients[39], suggesting an oncogenic function for YY1 in human B-cell lymphomagenesis. The Smurf2-YY1-c-Myc regulatory axis is thus a useful prognostic predictor of clinical outcome in DLBCL patients and a potential therapeutic target for treatment of DLBCL.

There is no evidence that the *Smurf2* locus is deleted in human DLBCL[40, 41] or Burkitt's lymphoma[42, 43], suggesting that epigenetic regulation probably plays an important role in Smurf2 deficiency in human lymphomagenesis. Moreover, we showed that restoration of Smurf2 expression in human DLBCL cells can suppress cell proliferation (Fig. 8f), providing an opportunity to design strategies to increase the expression of Smurf2 in lymphomas as a new therapeutic approach complementing current CHOP/R-CHOP regimens.

Increased susceptibility to B-cell lymphomagenesis in Smurf2-deficient mice is preceded by enhanced proliferation in splenic B cells. B cells undergo SHM and CSR in GCs to generate high-affinity antibodies. Both SHM and CSR are mutagenic and may target non-immunoglobulin genes. These "off-target" genetic alterations contribute to lymphomagenesis[2, 3, 4, 5, 6, 7, 8]. Enhanced proliferation would predispose Smurf2-deficient B cells to these mutagenic events, which ultimately contribute to lymphomagenesis. Consistent with this notion, Smurf2-deficient mice develop lymphomas at 12–15 months of age, most likely reflecting the infrequent generation of splenic GCs in un-immunized mice along with the accumulation of mutations with age. Recently it has been shown that Smurf2 regulates histone H2B monoubiquitination by targeting ring finger protein 20 (RNF20) for ubiquitination and degradation. Loss of Smurf2 leads to genomic instability through alterations in histone modification[15], suggesting an important mechanism through which Smurf2 functions as a tumor suppressor. Our work now adds a novel dimension to the tumor suppressive functions of Smurf2.

As YY1 has been shown to transactivate *c-Myc* expression[23, 24], our discovery of Smurf2-mediated ubiquitination and degradation of YY1 provides a novel mechanism by which Smurf2 regulates c-Myc expression and cell proliferation. *Myc* translocation is not common in DLBCL (5–10%), however, increased *Myc* expression is observed in ~30% of DLBCL and correlates with poor survival prognosis in DLBCL patients[44]. While no *IgH-Myc* translocation was found, lymphomas derived from Smurf2-deficient mice all showed increased expression of *c-Myc*. The Smurf2-YY1-c-Myc axis identified in the present study provides a plausible mechanism for increased *Myc* expression without chromosomal translocation in DLBCL.

As a master regulator of cell proliferation[45], the oncogenic function of c-Myc in B-cell lymphomagenesis is well documented[19, 20, 21, 46]. In response to activated oncogenes, intrinsic tumor suppression mechanisms such as apoptosis and senescence are triggered to restrain oncogenic proliferation. With c-Myc, an additional layer of complexity is provided by the exquisite sensitivity of cells to different levels of c-Myc overexpression. High level of c-Myc overexpression increases cell proliferation and drives lymphomagenesis, but also induces apoptosis[20, 21, 47]. Suppression of apoptosis exacerbates c-Myc-induced lymphomagenesis, suggesting that apoptosis antagonizes c-Myc's oncogenic activity[21]. Further, it has been recently found that low level of c-Myc elevation promotes cell proliferation without inducing apoptosis[48]. Consistent with this observation, we found that Smurf2-deficient mice showed low level (~2-fold) of c-Myc elevation (Fig. 5b) and enhanced proliferation in B cells without significant induction of apoptosis (Fig. 4 and Supplementary Fig. S7). In the absence of apoptosis, senescence likely becomes the critical

tumor suppression mechanism to antagonize the oncogenic activity of Myc. A recent study shows that constitutive activation of c-Myc indeed activates senescence[49]. Smurf2 is an important regulator of senescence[16, 50, 51, 52]. In Smurf2-deficient cells, impaired senescence response leads to prolonged cell proliferation including in splenic cells[16], suggesting that enhanced cell proliferation induced by low level of c-Myc activation coupled with an impaired senescence response drives lymphomagenesis in Smurf2-deficient mice. Smurf2 thus plays multiple roles in tumor suppression by maintaining chromatin landscape and genomic stability, suppressing cell proliferation and regulating the senescence response.

Methods

Smurf2-deficient mice

Smurf2-deficient mice as described previously[16] have been backcrossed to C57BL/6 for >10 generations. Tissues were harvested for DNA, RNA and protein preparation, or fixed in 10% phosphate-buffered formalin. 5-μm paraffin sections were stained for Hematoxylin & Eosin, PNA (Vector Labs), TUNEL (Roche), B220 and Ki-67 (antibody sources and dilutions in Supplementary Table S2). For transplantation, 2×10^6 splenic cells from tumor-bearing mice were injected retro-orbitally into sub-lethally irradiated (3 Gy) *Rag1*$^{-/-}$ mice (Jackson Laboratories). All studies were carried out according to guidelines approved by the Institutional Animal Care and Use Committee of University of Massachusetts Medical School.

Flow cytometry

Spleens were collected from 2-month old mice of both sexes and ground between frosted glass slides. Bone marrow cells were harvested from long leg bones. After red blood cells were lysed, cells were filtered through 70-μm nylon mesh and incubated with anti-CD16/32 antibody (10 min on ice). Cells were incubated with primary antibodies for 20 min and washed three times with staining media (biotin-, flavin-, and phenol red-deficient RPMI-1640 medium with 10 mM pH7.2 HEPES, 0.02% sodium azide, 1 mM EDTA and 2% FBS). Antibodies (sources and dilutions in Supplementary Table S3) included B220-APC (RA3-6B2), CD19-PE-TR (ID3), CD21-FITC (7G6), CD23-biotin (B3B4), CD24-FITC (30-F1), CD43-PE (S7), CD93-PE-Cy7 (AA4.1), CD95-PE (15A7), CD117(c-kit)-PE-Cy5.5 (2B8), CD127-PE (A7R34), IgD-PE or -biotin (11–26), IgM-APC, -biotin or -PE-Cy7 (II/41), IgG2a-PE (m2a-15F8) and Ly6C-FITC (AL21). Biotin-stained cells were incubated with streptavidin-pacific blue (Invitrogen) for 15 min on ice, washed three times and resuspended in 1 μg/ml propidium iodide to exclude dead cells. Flow cytometry was performed on 5-laser, 18-detector LSR II (BD Biosciences), and data were analyzed using FlowJo (Treestar).

Splenic B-cell proliferation assays

Mouse spleen was collected and processed as described above. Single splenic cell suspension was treated with 10 μM carboxyfluorescein succinimidyl ester (Invitrogen) for 10 min at 37°C, and cultured in RPMI-1640 medium with 10% FBS, 100 μM MEM non-essential amino acids, 2 mM glutamine, and 50 μM 2-mercaptoethanol (Invitrogen)in a humidified chamber containing 5% CO_2 at 37°C. Cells were treated with 5 μM

lipopolysaccharide (Sigma) or left untreated. Cells were stained with anti-B220-APC antibody daily for 4 days. After being washed and re-suspended in 1 μg/ml propidium iodide, cells were analyzed by flow cytometry with BD FACSCaliber and FlowJo.

Mice were injected with 1 mg bromodeoxyuridine (BrdU, BD Biosciences) intraperitoneally. Spleen was collected 24 hours later and processed as described above. Splenic cells were fixed, and stained with anti-BrdU-FITC antibody using BrdU flow kit (BD Biosciences) and anti-B220-APC antibody. Data were collected by flow cytometry on BD FACSCaliber and analyzed using FlowJo.

Cycloheximde treatment

Mouse splenic cells were harvested and cultured as described above. Cells were treated with 15 μg/ml cycloheximide (Sigma), and cell lysates were collected every 2 hours post treatment.

Class switch recombination and somatic hypermutation assays

Transcripts of mouse *IgH* were amplified by quantitative RT-PCR as described[53]. Briefly, μ (IgM) transcripts were amplified using primers ImF and CmR. Post-switch transcripts were amplified using the following primers: ImF and Cg1R for γ1 (IgG1), ImF and Cg2aR for γ2a (IgG2a), ImF and Cg2bR for γ2b (IgG2b), ImF and Cg3R for γ3 (IgG3). Primers used are ImF: 5′-CTCTGGCCCTGCTTATTGTTG-3′; CmR: 5′-GAAGACATTTGGGAAGGACTGACT-3′; Cg1R: 5′-GGATCCAGAGTTCCAGGTCACT-3′; Cg2aR: 5′-GCCACATTGCAGGTGATGGA-3′; Cg2bR: 5′-CACTGAGCTGCTCATAGTGTAGAGTC-3′; and Cg3R: 5′-CTCAGGGAAGTAGCCTTTGACA-3′.

The frequency of somatic mutation in mouse *IgH* was determined as described[53]. Briefly, V_H186.2 transcripts of mouse *IgH* μ isotype were amplified in RT-PCR using Phusion hot start high-fidelity Taq Polymerase (New England Biolabs) with primers V_H186.2 (5′-TTCTTGGCAGCAACAGCTACA-3′) and CmR (5′-GAAGACATTTGGGAAGGACTGACT-3′). PCR products were cloned into pGEM-T-easy vector (Promega), and individual colonies were sequenced.

Clonal analysis of mouse B-cell lymphomas

Rearrangements of the variable region of mouse *IgH* were analyzed as described[54]. Briefly, genomic DNA was prepared from lymphoma-bearing spleen of Smurf2-deficient mice or spleen of wild-type mice using classic genomic DNA isolation kit (LamdaBiotech), and used in PCR with primers V_H (J558FR3: 5′-CAGCCTGACATCTGAGGACTCTGC-3′) and 3′ of J_{H4} (JH4int: 5′-CTCCACCAGACCTCTCTAGACAGC-3′).

Analysis of *IgH-Myc* translocation

IgH-Myc translocation in mouse B-cell lymphomas was detected as described[55]. Briefly, genomic DNA isolated from lymphomas was used as template in nested PCR using expended long PCR system (Roche). Primers were: 5′-TGAGGACCAGAGAGGGATAAAAGAGAA-3′ and 5′-

GGGGAGGGGGTGTCAAATAATAAGA-3′ (1st round); 5′-CACCCTGCTATTTCCTTGTTGCTAC-3′and 5′-GACACCTCCCTTCTACACTCTAAACCG-3′ (2nd round). *Myc* locus was amplified as controls with primers of 5′-GGGGAGGGGGTGTCAAATAATAAGA-3′ and 5′-GTGAAAACCGACTGTGGCCCTGGAA-3′. Two lymphoma samples (318 and 334) with *IgH-Myc* translocation[56] were kindly provided by Dr. John Manis (Harvard Medical School) and used as positive controls.

Cell culture and transfection

SUDHL-6 cells (kindly provided by Dr. Subbarao Bondada, University of Kentucky) werecultured in RPMI-1640 medium with 10% FBS in a humidified chamber containing 5%CO_2 at 37°C. Lentiviral vectors pLenti-CMV-Smurf2-IRES-Puro, pLenti-CMV-C716A-IRES-Puro or pLenti-CMV-GFP-IRES-Puro were described previously[51]. Briefly, fragments of Smurf2 or GFP cDNA were inserted ito a lentiviral vector to express Smurf2 or GFP under the control of a CMV promoter. Lentiviral shRNA constructs targeting Smurf2 (V2LHS_10399), YY1 (V2LHS_219592, V2LHS_389741) and a non-silencing shRNA control (RHS4346) were purchased from Open Biosystems. Lentiviral packaging and infection were carried out as described[51]. Briefly, Lentiviral vectors were co-transfected with a plasmid (pMD2. VSV-G) encoding vesicular stomatitis virus glycoprotein (VSV-G) and a plasmid (pCMVdR8.74) encoding packaging proteins into 293T cells. VSV-G pseudotyped virus were collected 48 hr after transfection and used to infected target cells in the presence of 4 μg/ml polybrene (Sigma). Cells were FACS sorted for GFP+ cells (shRNA knockdown) or selected with puromycin (1 μg/ml, Sigma) for 1 week.

To analyze cell proliferation, sorted or selected cells were seeded at 5×10^3 per well in 6-well plates, harvested in triplicate and counted daily for 5 days using Z1Coulter Particle Counter (Beckman Coulter). Apoptosis was measured using Caspase-Glo 3/7 assay (Promega).

Splenic B cells were isolated using anti-B220-biotin antibody and anti-biotin beads with AutoMACS Pro (Miltenyi Biotec) and cultured with 5 μM LPS as described above. 3×10^6 cells were transfected with 10 pmol YY1 siRNA (sc-36864) or control siRNA (sc-37007, Santa Cruz Biotechnology) using mouse B cell Nucleofector kit on Nucelofector I device (Lonza) with program Z-01. Cell lysates were collected 48 hours after transfection.

Quantitative RT-PCR

Total RNA was isolated using RNeasy Mini kit (Qiagen) and reverse-transcribed using Superscript II (Invitrogen). Real-time PCR was performed using SYBR Green PCR kit (Bio-Rad). The following primers were used: Smurf2 (F: 5′-ATGAAGTCATTCCCCAGCAC-3′; R: 5′-AACCGTGCTCGTCTCTCTTC-3′), c-Myc (F: 5′-GGACAGTGTTCTCTGCC-3′; R: 5′-CGTCGCAGATGAAATAGG-3′), YY1 (F: 5′-TGAGAAAGCATCTGCACACC-3′; R: 5′-CGCAAATTGAAGTCCAGTGA-3′), Apex1 (F: 5′-GCTCCGTCAGACAAAGAAGG-3′; R: 5′-GCATTGGGAACATAGGCTGT-3′), Cad (F: 5′-TGGTCAGTTCATCCTCACTCC-3′; R: 5′-TACATGCCGTTCTCAGCTTG-3′), Ncl (F: 5′-TAAGGGTGAAGGTGGCTTTG-3′; R: 5′-CCTTGTGGCTTGAAGTCTCC-3′) and β-actin (F: 5′-GCTCTTTTCCAGCCTTCCTT-3′; R: 5′-GTGCTAGGAGCCAGAGCAGT-3′).

Western blot and co-immunoprecipitation analysis

Total cell lysates were collected using RIPA buffer (50 mM Tris–HCl pH 7.5, 150 mMNaCl, 1% Triton X-100, 0.1% SDS, 0.5% deoxycholic acid, 0.02% sodium azide) with freshly added complete protease inhibitors (Roche). Protein lysates (20 μg) were separated by SDS–PAGE Criterion X-gel (Bio-Rad) and transferred to nitrocellulose membranes (GE Osmonics). Immunoblots were analyzed by Western blotting and visualized using a Western lightening chemiluminescence detection kit (PerkinElmer). Primary antibodies were Smurf2, c-Myc, YY1, Flag, HA, ubiquitin, β-actin and GAPDH (antibody sources and dilutions in Supplementary Table S2). For co-immunoprecipitation, cells were lysed in NP40 lysis buffer (20 mM Tris–HCl, 150 mM NaCl, 2 nM EDTA, 1% Nonidet P-40) plus complete protease inhibitors (Roche). Lysates were incubated with anti-Flag M2 affinity gel (Sigma) overnight at 4°C. Immunoprecipitates were washed four times with NP40 lysis buffer, and analyzed in Western blot with anti-HA antibody.

Ubiquitination assay

293T cells were transfected with HA-YY1 (a gift of Dr. Yang Shi, Harvard Medical School), 3xFlag-ubiquitin (provided by Dr. Quan Lu, Harvard School of Public Health) and Smurf2. GFP and C716A were used as controls. Cells were treated with MG132 (20 μM, Sigma) for 2 hours and lysed in RIPA buffer (50 mM Tris–HCl pH 7.5, 150 mM NaCl, 1% Triton X-100, 0.1% SDS, 0.5% deoxycholic acid, 0.02% sodium azide) plus 10 mM *N*-ethylmaleimide (Fisher Scientific). Cell lysates were incubated with anti-HA or anti-Flag affinity gel (Sigma) overnight at 4°C. Immunoprecipitates were washed with RIPA buffer three times, and analyzed in Western blot with anti-Flag or anti-HA antibody to detect ubiquitin conjugation. To detect ubiquitination of endogenous YY1 in SUDHL-6 cells, cell lysates were incubated with anti-YY1 antibody overnight at 4°C followed by incubation with protein A-agarose (Invitrogen). Poly-ubiquitinated YY1 was detected in Western blot using anti-ubiquitin antibody.

Chromatin immunoprecipitation assay

Mouse spleen was collected and processed as described above. Single cell suspension was cross-linked using 1% formaldehyde (Sigma) in RPMI-1640 medium (room temperature for 10 min). After neutralization with glycine (125 nM), cells were lysed in SDS lysis buffer. Chromatin was sonicated to fragments of ~500 bp, and Chromatin immunoprecipitation (ChIP) with anti-YY1 antibody or matched IgG was performed using ChromaFlash one step ChIP kit (Epigentek). After reverse of cross-linking (65°C for 3 hours), the *c-Myc* promoter region containing the YY1 binding site was amplified in quantitative PCR with primers: F: 5′-TCCCCAGCCTTAGAGAGACG-3′ and R: 5′-GGCTCCGGGGTGTAAACAGT-3′. Chromatin before ChIP was used as input.

Gene expression and statistical analyses

Microarray data (GSE2350, GSE4475 and GSE10846) were retrieved from GEO(http://www.ncbi.nil.nih.gov/geo). Expression of Smurf2 ($\log_2$ transformed) was analyzedwith dot plot, and one-way ANOVA was used for statistical analysis. Kaplan-Meier survival curves were plotted using GraphPad Prism 5.0, and log-rank test was used for statistical analysis.

Univariate and multivariate Cox regression analyses were used to estimate the hazard ratios and 95% confidence intervals, and statistical significance was analyzed using SPSS Statistics 19 software (IBM).

Human DLBCL dataset GSE10846 contains samples from patients receiving CHOP or R-CHOP treatment. Revised International Prognostic Index (IPI) score was used to group these patients: low (0), intermediate (1 or 2) or high (3, 4 or 5)[34]. Some IPI variables were missing in some samples. If the missing IPI variables did not change the IPI grouping of a given sample, this sample was included in the analysis. Otherwise, the sample was excluded.

Data were presented as mean ± SD. Two-tailed and unpaired Student *t*-test was used for pairwise comparisons, with $P<0.05$ considered as statistically significant.

Supplementary Material

Refer to Web version on PubMed Central for supplementary material.

Acknowledgments

We thank Dr. John Manis for IgH and IgH-Myc PCR protocols, reagents and helpful discussion; Drs. Subbarao Bondada, Quan Lu, Madelyn Schmidt, Yang Shi, Janet Stavnezer and Robert Woodland for kindly providing reagents; Dr. Suyang Hao for pathological diagnosis of lymphoma samples; Dr. Madelyn Schmidt for advice on LPS stimulation and CFSE staining; Erin Cloherty and Laura Fineman for technical assistance. This work was supported by grants from the National Cancer Institute (R01CA131210) and The Ellison Medical Foundation (AG-NS-0347-06) to H.Z.

References

1. Victora GD, Nussenzweig MC. Germinal centers. Annu Rev Immunol. 2012; 30:429–457. [PubMed: 22224772]
2. Pasqualucci L, et al. BCL-6 mutations in normal germinal center B cells: evidence of somatic hypermutation acting outside Ig loci. Proc Natl Acad Sci U S A. 1998; 95:11816–11821. [PubMed: 9751748]
3. Pasqualucci L, et al. Hypermutation of multiple proto-oncogenes in B-cell diffuse large-cell lymphomas. Nature. 2001; 412:341–346. [PubMed: 11460166]
4. Staszewski O, Baker RE, Ucher AJ, Martier R, Stavnezer J, Guikema JE. Activation-induced cytidine deaminase induces reproducible DNA breaks at many non-Ig Loci in activated B cells. Mol Cell. 2011; 41:232–242. [PubMed: 21255732]
5. Robbiani DF, et al. AID is required for the chromosomal breaks in c-myc that lead to c-myc/IgH translocations. Cell. 2008; 135:1028–1038. [PubMed: 19070574]
6. Robbiani DF, et al. AID produces DNA double-strand breaks in non-Ig genes and mature B cell lymphomas with reciprocal chromosome translocations. Mol Cell. 2009; 36:631–641. [PubMed: 19941823]
7. Shen HM, Peters A, Baron B, Zhu X, Storb U. Mutation of BCL-6 gene in normal B cells by the process of somatic hypermutation of Ig genes. Science. 1998; 280:1750–1752. [PubMed: 9624052]
8. Liu M, et al. Two levels of protection for the B cell genome during somatic hypermutation. Nature. 2008; 451:841–845. [PubMed: 18273020]
9. Allen CD, Okada T, Cyster JG. Germinal-center organization and cellular dynamics. Immunity. 2007; 27:190–202. [PubMed: 17723214]
10. Lenz G, Staudt LM. Aggressive lymphomas. N Engl J Med. 2010; 362:1417–1429. [PubMed: 20393178]

11. A clinical evaluation of the International Lymphoma Study Group classification of non-Hodgkin's lymphoma. The Non-Hodgkin's Lymphoma Classification Project. Blood. 1997; 89:3909–3918. [PubMed: 9166827]
12. Schneider C, Pasqualucci L, Dalla-Favera R. Molecular pathogenesis of diffuse large B-cell lymphoma. Semin Diagn Pathol. 2011; 28:167–177. [PubMed: 21842702]
13. Nogai H, Dorken B, Lenz G. Pathogenesis of non-Hodgkin's lymphoma. J Clin Oncol. 2011; 29:1803–1811. [PubMed: 21483013]
14. Coiffier B. Diffuse large cell lymphoma. Curr Opin Oncol. 2001; 13:325–334. [PubMed: 11555708]
15. Blank M, Tang Y, Yamashita M, Burkett SS, Cheng SY, Zhang YE. A tumor suppressor function of Smurf2 associated with controlling chromatin landscape and genome stability through RNF20. Nat Med. 2012; 18:227–234. [PubMed: 22231558]
16. Ramkumar C, et al. Smurf2 regulates the senescence response and suppresses tumorigenesis in mice. Cancer Res. 2012; 72:2714–2719. [PubMed: 22552287]
17. Green MR, et al. Signatures of murine B-cell development implicate Yy1 as a regulator of the germinal center-specific program. Proc Natl Acad Sci U S A. 2011; 108:2873–2878. [PubMed: 21282644]
18. Morse HC 3rd, et al. Bethesda proposals for classification of lymphoid neoplasms in mice. Blood. 2002; 100:246–258. [PubMed: 12070034]
19. Dalla-Favera R, Martinotti S, Gallo RC, Erikson J, Croce CM. Translocation and rearrangements of the c-myc oncogene locus in human undifferentiated B-cell lymphomas. Science. 1983; 219:963–967. [PubMed: 6401867]
20. Langdon WY, Harris AW, Cory S, Adams JM. The c-myc oncogene perturbs B lymphocyte development in E-mu-myc transgenic mice. Cell. 1986; 47:11–18. [PubMed: 3093082]
21. Soucek L, Evan GI. The ups and downs of Myc biology. Curr Opin Genet Dev. 2010; 20:91–95. [PubMed: 19962879]
22. Zeller KI, Jegga AG, Aronow BJ, O'Donnell KA, Dang CV. An integrated database of genes responsive to the Myc oncogenic transcription factor: identification of direct genomic targets. Genome Biol. 2003; 4:R69. [PubMed: 14519204]
23. Riggs KJ, et al. Yin-yang 1 activates the c-myc promoter. Mol Cell Biol. 1993; 13:7487–7495. [PubMed: 8246966]
24. Hsu KW, et al. The activated Notch1 receptor cooperates with alpha-enolase and MBP-1 in modulating c-myc activity. Mol Cell Biol. 2008; 28:4829–4842. [PubMed: 18490439]
25. Kavsak P, et al. Smad7 binds to Smurf2 to form an E3 ubiquitin ligase that targets the TGF beta receptor for degradation. Mol Cell. 2000; 6:1365–1375. [PubMed: 11163210]
26. Lin X, Liang M, Feng XH. Smurf2 is a ubiquitin E3 ligase mediating proteasome-dependent degradation of Smad2 in transforming growth factor-beta signaling. J Biol Chem. 2000; 275:36818–36822. [PubMed: 11016919]
27. Zhang Y, Chang C, Gehling DJ, Hemmati-Brivanlou A, Derynck R. Regulation of Smad degradation and activity by Smurf2, an E3 ubiquitin ligase. Proc Natl Acad Sci U S A. 2001; 98:974–979. [PubMed: 11158580]
28. Basso K, Margolin AA, Stolovitzky G, Klein U, Dalla-Favera R, Califano A. Reverse engineering of regulatory networks in human B cells. Nat Genet. 2005; 37:382–390. [PubMed: 15778709]
29. Hummel M, et al. A biologic definition of Burkitt's lymphoma from transcriptional and genomic profiling. N Engl J Med. 2006; 354:2419–2430. [PubMed: 16760442]
30. Lenz G, et al. Stromal gene signatures in large-B-cell lymphomas. N Engl J Med. 2008; 359:2313–2323. [PubMed: 19038878]
31. Dave SS, et al. Prediction of survival in follicular lymphoma based on molecular features of tumor-infiltrating immune cells. N Engl J Med. 2004; 351:2159–2169. [PubMed: 15548776]
32. Alizadeh AA, et al. Distinct types of diffuse large B-cell lymphoma identified by gene expression profiling. Nature. 2000; 403:503–511. [PubMed: 10676951]

33. Wright G, Tan B, Rosenwald A, Hurt EH, Wiestner A, Staudt LM. A gene expression-based method to diagnose clinically distinct subgroups of diffuse large B cell lymphoma. Proc Natl Acad Sci U S A. 2003; 100:9991–9996. [PubMed: 12900505]
34. Sehn LH, et al. The revised International Prognostic Index (R-IPI) is a better predictor of outcome than the standard IPI for patients with diffuse large B-cell lymphoma treated with R-CHOP. Blood. 2007; 109:1857–1861. [PubMed: 17105812]
35. Castellano G, et al. The involvement of the transcription factor Yin Yang 1 in cancer development and progression. Cell Cycle. 2009; 8:1367–1372. [PubMed: 19342874]
36. Shi Y, Lee JS, Galvin KM. Everything you have ever wanted to know about Yin Yang 1. Biochim Biophys Acta. 1997; 1332:F49–66. [PubMed: 9141463]
37. Liu H, et al. Yin Yang 1 is a critical regulator of B-cell development. Genes Dev. 2007; 21:1179–1189. [PubMed: 17504937]
38. Castellano G, et al. Yin Yang 1 overexpression in diffuse large B-cell lymphoma is associated with B-cell transformation and tumor progression. Cell Cycle. 2010; 9:557–563. [PubMed: 20081364]
39. Sakhinia E, et al. Clinical quantitation of diagnostic and predictive gene expression levels in follicular and diffuse large B-cell lymphoma by RT-PCR gene expression profiling. Blood. 2007; 109:3922–3928. [PubMed: 17255358]
40. Lenz G, et al. Molecular subtypes of diffuse large B-cell lymphoma arise by distinct genetic pathways. Proc Natl Acad Sci U S A. 2008; 105:13520–13525. [PubMed: 18765795]
41. Bea S, et al. Diffuse large B-cell lymphoma subgroups have distinct genetic profiles that influence tumor biology and improve gene-expression-based survival prediction. Blood. 2005; 106:3183–3190. [PubMed: 16046532]
42. Salaverria I, et al. Chromosomal alterations detected by comparative genomic hybridization in subgroups of gene expression-defined Burkitt's lymphoma. Haematologica. 2008; 93:1327–1334. [PubMed: 18698080]
43. Scholtysik R, et al. Detection of genomic aberrations in molecularly defined Burkitt's lymphoma by array-based, high resolution, single nucleotide polymorphism analysis. Haematologica. 2010; 95:2047–2055. [PubMed: 20823134]
44. Horn H, et al. MYC status in concert with BCL2 and BCL6 expression predicts outcome in diffuse large B-cell lymphoma. Blood. 2013; 121:2253–2263. [PubMed: 23335369]
45. Dang CV. MYC, microRNAs and glutamine addiction in cancers. Cell Cycle. 2009; 8:3243–3245. [PubMed: 19806017]
46. Harris AW, Pinkert CA, Crawford M, Langdon WY, Brinster RL, Adams JM. The E mu-myc transgenic mouse. A model for high-incidence spontaneous lymphoma and leukemia of early B cells. J Exp Med. 1988; 167:353–371. [PubMed: 3258007]
47. Evan G, Littlewood T. A matter of life and cell death. Science. 1998; 281:1317–1322. [PubMed: 9721090]
48. Murphy DJ, et al. Distinct thresholds govern Myc's biological output in vivo. Cancer Cell. 2008; 14:447–457. [PubMed: 19061836]
49. Campaner S, et al. Cdk2 suppresses cellular senescence induced by the c-myc oncogene. Nat Cell Biol. 2010; 12:54–59. 51–14. [PubMed: 20010815]
50. Zhang H, Cohen SN. Smurf2 up-regulation activates telomere-dependent senescence. Genes Dev. 2004; 18:3028–3040. [PubMed: 15574587]
51. Zhang H, Teng Y, Kong Y, Kowalski PE, Cohen SN. Suppression of human tumor cell proliferation by Smurf2-induced senescence. J Cell Physiol. 2008; 215:613–620. [PubMed: 18181147]
52. Kong Y, Cui H, Zhang H. Smurf2-mediated ubiquitination and degradation of Id1 regulates p16 expression during senescence. Aging Cell. 2011; 10:1038–1046. [PubMed: 21933340]
53. Muramatsu M, Kinoshita K, Fagarasan S, Yamada S, Shinkai Y, Honjo T. Class switch recombination and hypermutation require activation-induced cytidine deaminase (AID), a potential RNA editing enzyme. Cell. 2000; 102:553–563. [PubMed: 11007474]
54. Jolly CJ, Klix N, Neuberger MS. Rapid methods for the analysis of immunoglobulin gene hypermutation: application to transgenic and gene targeted mice. Nucleic Acids Res. 1997; 25:1913–1919. [PubMed: 9115357]

55. Kovalchuk AL, Muller JR, Janz S. Deletional remodeling of c-myc-deregulating chromosomal translocations. Oncogene. 1997; 15:2369–2377. [PubMed: 9393881]

56. Wang JH, et al. Oncogenic transformation in the absence of Xrcc4 targets peripheral B cells that have undergone editing and switching. J Exp Med. 2008; 205:3079–3090. [PubMed: 19064702]

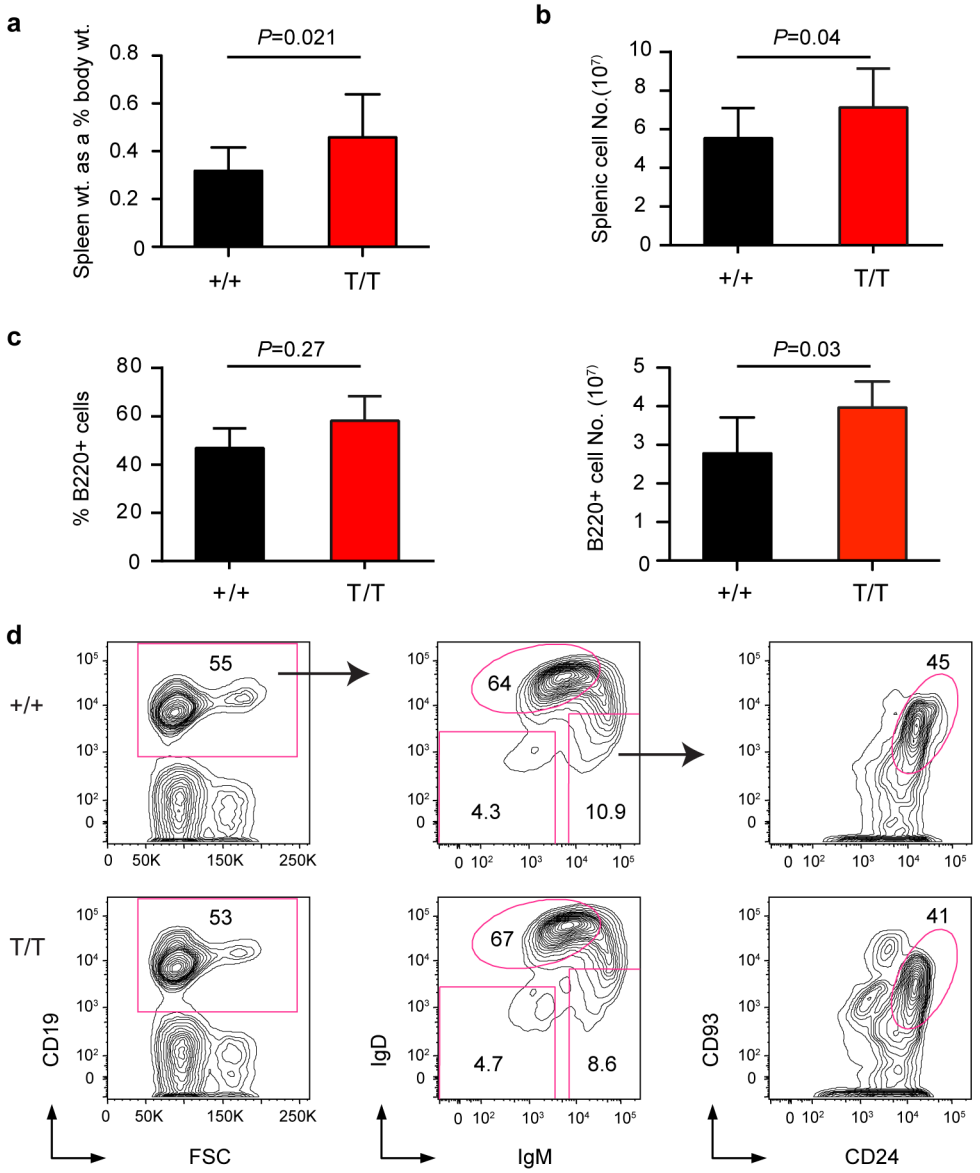

Figure 1. Characterization of splenic B cells

(**a**) Relative gross spleen weight to body weight of 2-month-old wild-type (+/+) and *Smurf2*$^{T/T}$ (T/T) mice (N=12). (**b**) Total live splenic cells (N=12) and (**c**) Percent and total live B220^{+} cells in spleens of 2-month-old wild-type and *Smurf2*$^{T/T}$ mice (N=6). Error bars in (**a-c**) are standard deviations. Student *t*-test is used for statistical analysis. (**d**) Representative FACS analysis of splenic B cells from 2-month-old wild-type and *Smurf2*$^{T/T}$ mice. Live cells (propidium iodide excluding) are displayed. The IgD^{++}IgM^{int} population, indicated by a circular gate in the middle panel, are follicular B cells. CD93^{+}CD24^{+} cells, indicated by a circular gate in the right panel, are immature B cells. Frequency of each gated population as a percent of displayed cells is shown.

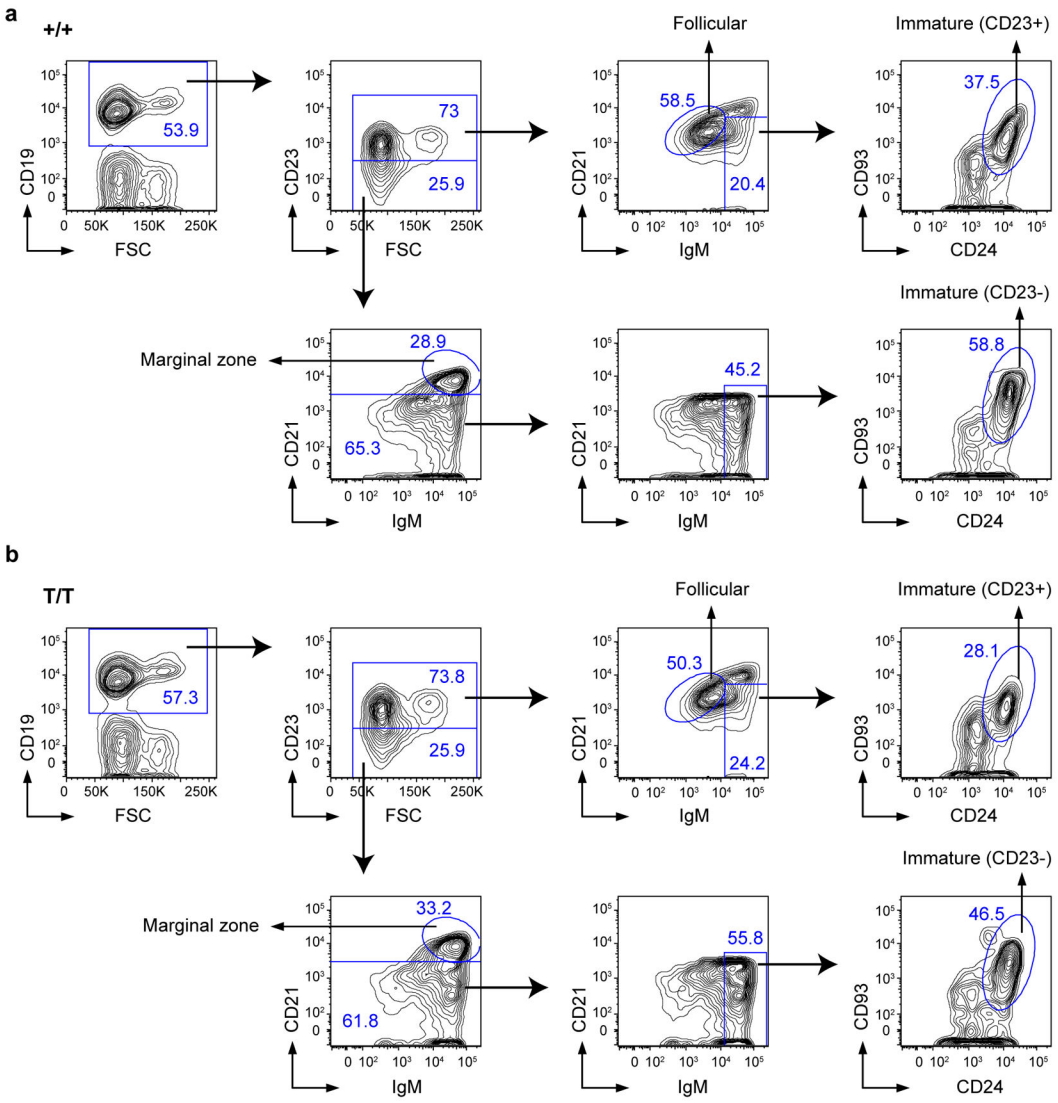

Figure 2. Characterization of B cells in the spleen of Smurf2-deficient mice

Representative FACS analysis of splenic cells from 2-month old (**a**) wild-type (+/+) and (**b**) *Smurf2*$^{T/T}$ (T/T) mice. Live cells (propidium iodide excluding) are displayed. Sequential gating strategies are indicated by arrows. Frequency of each gated population as a percent of displayed cells is shown.

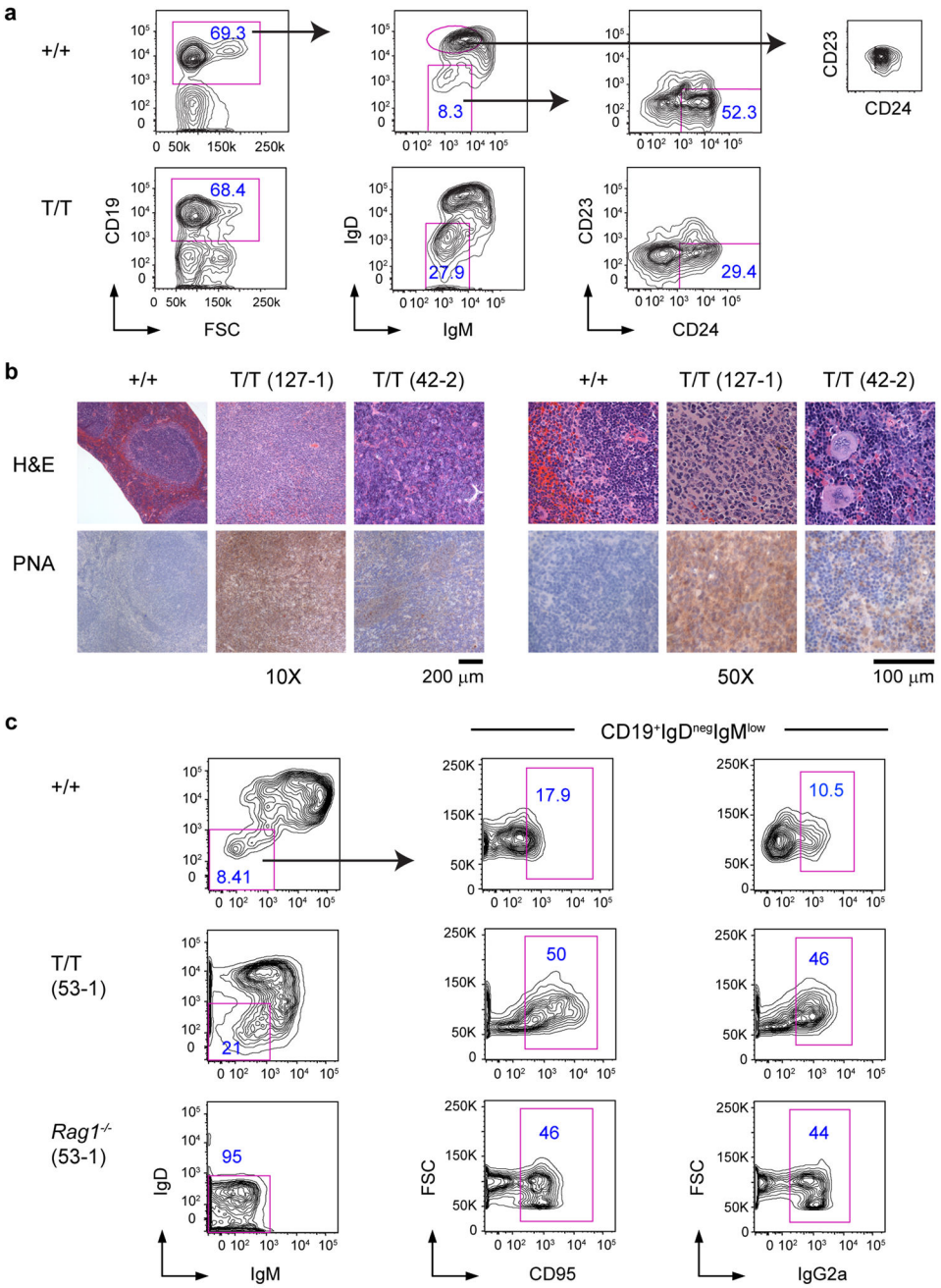

Figure 3. Characterization of B-cell lymphomas generated in Smurf2-deficient mice

(**a**) Representative FACS analysis of splenic cells from lymphoma-bearing *Smurf2*$^{T/T}$ (T/T) and age-matched wild-type (+/+) mice. Frequency of each gated population as a percent of displayed cells is shown. CD23^{-}CD24^{+} cells in the right panel are activated or previously activated B cells. The CD23 vs. CD24 plot for follicular B cells (IgD^{++}IgM^{int}) in wild-type mice is provided for comparison. (**b**) Representative H&E and PNA staining of lymphomas in spleen of *Smurf2*$^{T/T}$ mice and wild-type mouse spleen. Scale bars are 200 μm (10X) and 100 μm (50X). (**c**) Representative FACS analysis of CD19^{+} splenic B cells from a lymphoma-bearing *Smurf2*$^{T/T}$ mouse and a *Rag1*$^{-/-}$ recipient mouse injected with spleen

cells from this lymphoma-bearing mouse are presented. An age-matched wild-type mouse is analyzed as a control, and $CD19^{+}IgD^{neg}IgM^{low}$ population gated for CD95 or IgG2a is shown for comparison. Mice used in these studies were between 15 and 18 months of age.

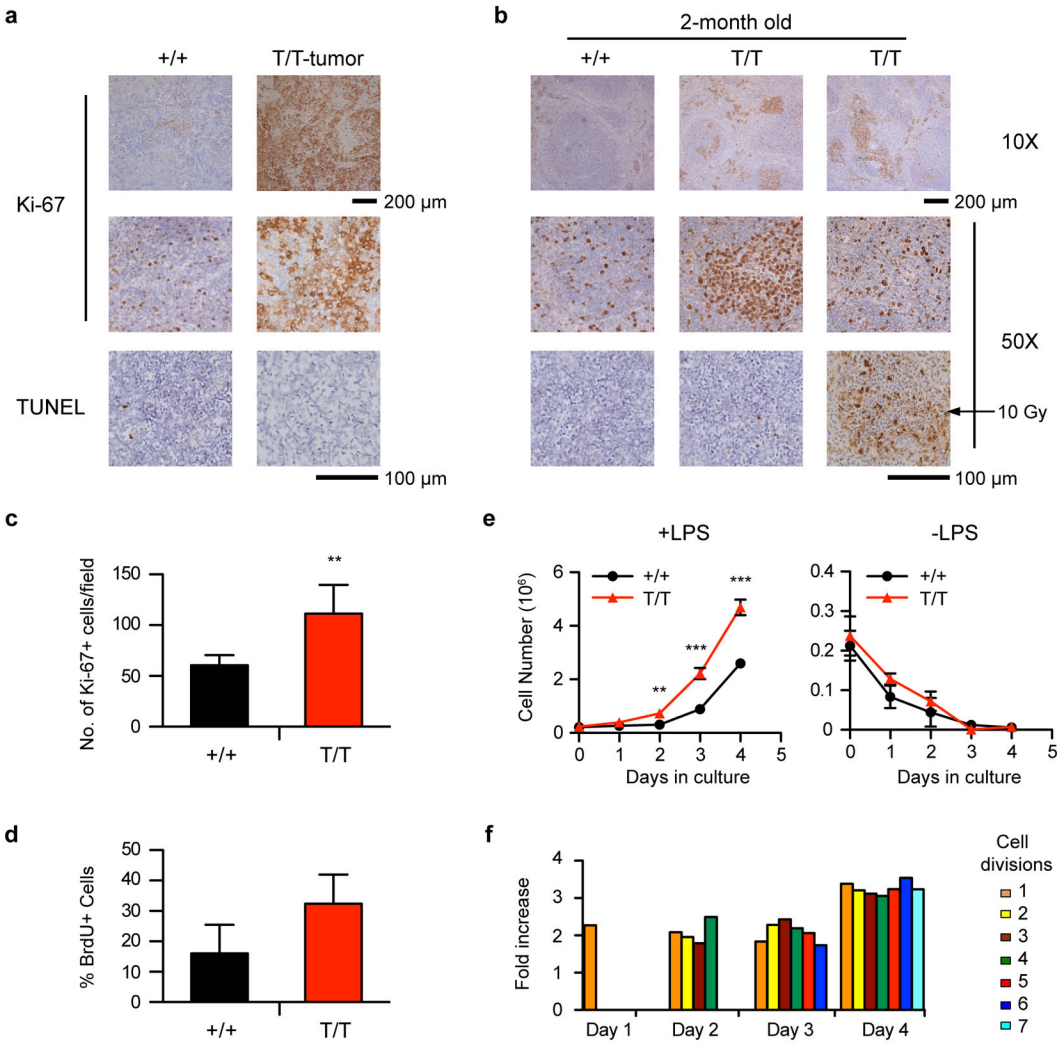

Figure 4. Enhanced proliferation of splenic B cells in Smurf2-deficient mice

(**a**) Representative Ki-67 and TUNEL staining of lymphomas in *Smurf2*$^{T/T}$ (T/T) mice. Staining of spleen sections of aged wild-type (+/+) mice is shown for comparison. (**b**) Representative Ki-67 and TUNEL staining of spleen sections of 2-month old wild-type and *Smurf2*$^{T/T}$ mice. TUNEL staining of spleen sections of an irradiated (10 Gy) mouse is shown for comparison. Scale bars are 200 μm (10X) and 100 μm (50X). (**c**) Quantitation of Ki-67 positive cells in 10 randomly selected fields in spleen sections of 2-month old wild-type and *Smurf2*$^{T/T}$ mice. (**d**) Analysis of BrdU incorporation in B220^{+} splenic cells of 2-month old wild-type and *Smurf2*$^{T/T}$ mice (N=3). (**e**) Splenic cells from 2-month old wild-type and *Smurf2*$^{T/T}$ mice are cultured with or without LPS. The number of B220^{+} viable cells (propidium iodide-negative) is determined by flow cytometry. Average of 3 independent experiments is shown. (**f**) The number of B220^{+} cells undergoing different numbers of cell division is determined by CFSE staining and flow cytometry. The ratio of the number of B220^{+} *Smurf2*$^{T/T}$ cells undergoing different cell divisions over that of wild-type cells in one representative experiment is presented. Error bars in (**c–e**) are standard deviations of at least

3 independent experiments. Student *t*-test is used to compare *Smurf2*$^{T/T}$ samples with wild-type samples. **: $P<0.01$ and ***: $P<0.001$.

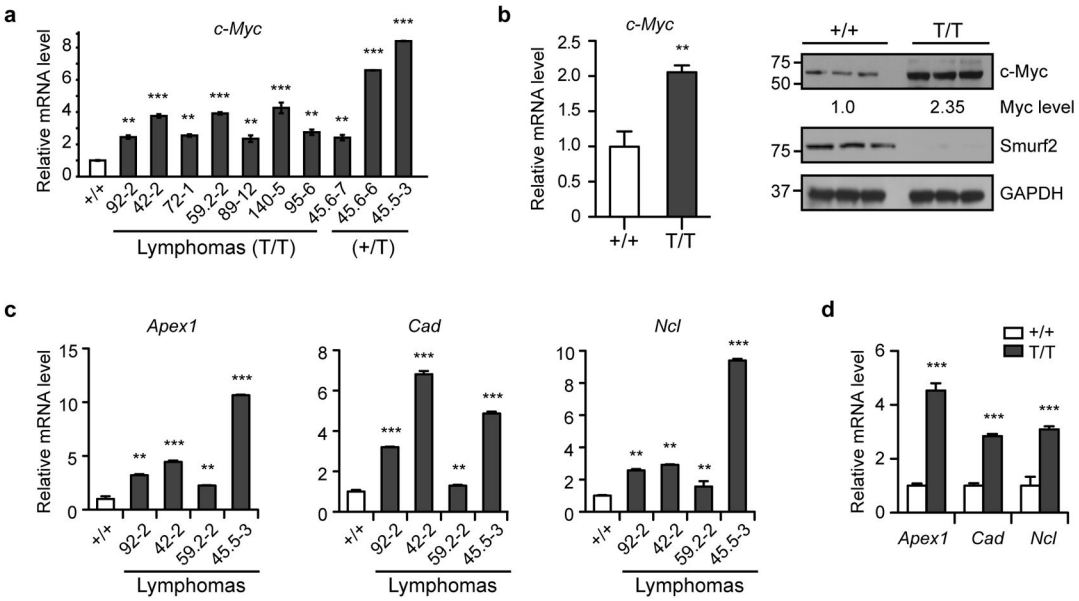

Figure 5. Elevated c-Myc expression in Smurf2-deficient mice

(**a**) Quantitative RT-PCR analysis of *c-Myc* expression in lymphomas in *Smurf2*$^{T/T}$ (T/T) or *Smurf2*$^{+/T}$ (+/T) mice compared with spleen of aged wild-type (+/+) mice. (**b**) Quantitative RT-PCR and Western analyses of c-Myc expression in spleen of 2-month old wild-type and *Smurf2*$^{T/T}$ mice. Larger images of immunoblots are shown in Supplementary Figure S11a. Quantitative RT-PCR analysis of c-Myc target genes in (**c**) representative lymphomas from *Smurf2*$^{T/T}$ mice compared with spleen of aged wild-type mice, and (**d**) spleen of 2-month old wild-type and *Smurf2*$^{T/T}$ mice. Error bars are standard deviations of 3 independent experiments. Student *t*-test is used to compare *Smurf2*$^{T/T}$ samples with wild-type samples. **: $P<0.01$ and ***: $P<0.001$.

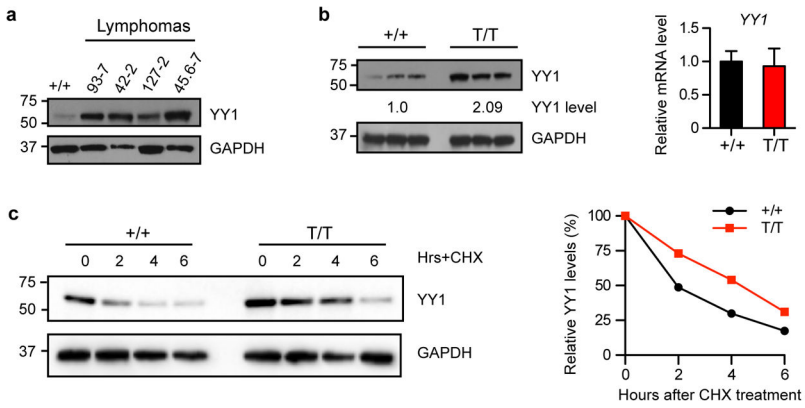

Figure 6. Smurf2 regulates the stability of YY1 protein

(**a**) Western analysis of YY1 expression in lymphomas compared with spleen of aged wild-type (+/+) mice. (**b**) Western and quantitative RT-PCR analyses of YY1 expression in spleens of 2-month old wild-type and *Smurf2*$^{T/T}$ (T/T) mice. Error bars are standard deviations of 3 independent experiments. (**c**) Stability of YY1 protein is determined in splenic B cells from 2-month old wild-type and *Smurf2*$^{T/T}$ mice after treatment with cycloheximide (CHX). The levels of YY1 protein at time 0 are set as 100%. Larger images of immunoblots are shown in Supplementary Figure S11b.

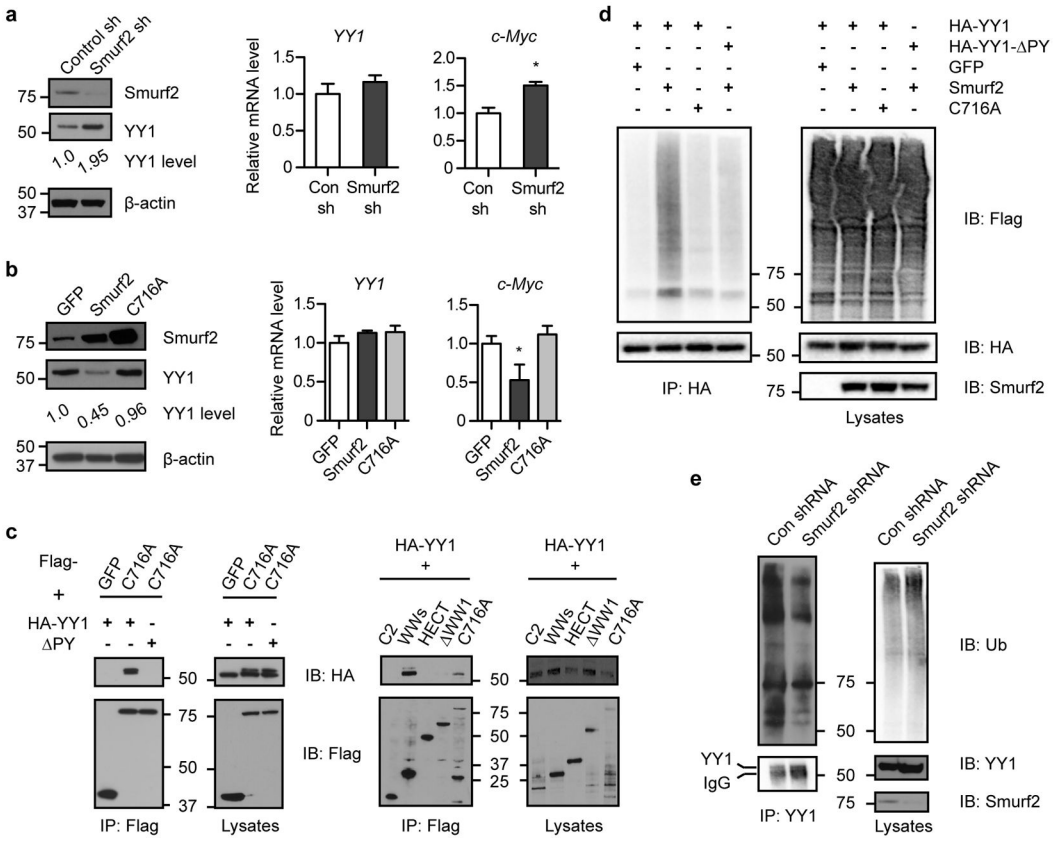

Figure 7. Smurf2 mediates ubiquitination of YY1

(**a**) Smurf2 expression is knocked down by shRNA or (**b**) Smurf2 or ligase mutant C716A is ectopically expressed in human DLBCL cells SUDHL-6. The expression of YY1 or c-Myc is analyzed in Western and quantitative RT-PCR. Error bars are standard deviations of 3 independent experiments. Student *t*-test is used for statistical analysis. *: $P<0.05$. (**c**) Smurf2 interacts with YY1. 293T cells are transfected with indicated constructs, and immunoprecipitation (IP) with anti-Flag antibody is followed by immunoblotting (IB) with anti-HA antibody. Larger images of immunoblots are shown in Supplementary Figure S11c and S12. (**d**) Smurf2 ubiquitinates YY1. 293T cells are transfected with HA-YY1 (or ΔPY), 3xFlag-Ub and Smurf2 (or C716A). IP with anti-HA antibody is followed by IB with anti-Flag antibody to detect poly-ubiquitinated YY1. (**e**) Down-regulation of Smurf2 by shRNA results in decreased ubiquitination of endogenous YY1 in human DLBCL cell line SUDHL-6. IP with anti-YY1 antibody is followed by IB with anti-ubiquitin antibody to detect poly-ubiquitinated YY1. Larger images of immunoblots are shown in Supplementary Figure S13a.

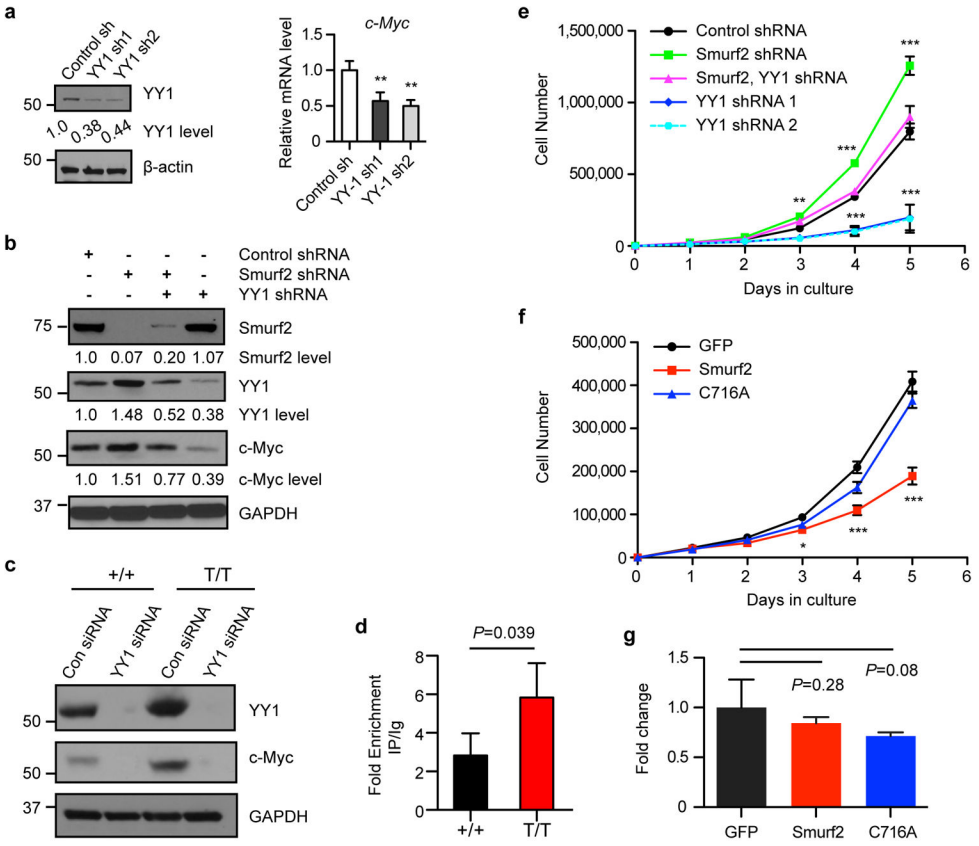

Figure 8. Smurf2-YY1 regulates c-Myc expression and cell proliferation

(**a**) Down-regulation of YY1 by shRNA (left image) leads to decreased c-Myc in human DLBCL cell line SUDHL-6 as determined by quantitative RT-PCR (right image). (**b**) Western analysis of c-Myc expression in SUDHL-6 cells after shRNA-mediated knockdown of *Smurf2* or *YY1* expression. (**c**) Knockdown of *YY1* by siRNA leads to down-regulation of c-Myc in splenic B cells of wild-type (+/+) and $Smurf2^{T/T}$ (T/T) mice. (**d**) Chromatin immunoprecipitation (ChIP) assay of YY1 binding onto the *c-Myc* promoter in spleens of 2-month old wild-type and $Smurf2^{T/T}$ mice. Fold enrichment of ChIP with anti-YY1 antibody over IgG control is shown. (**e**) Growth curves of human DLBCL cell line SUDHL-6 after shRNA-mediated knockdown of *Smurf2* or *YY1* expression. (**f**) Growth curves and (**g**) apoptosis assay of SUDHL-6 cells after ectopic expression of Smurf2, ligase mutant C716A or GFP control. Error bars are standard deviations of 3 independent experiments. Cells with shRNA knockdown or Smurf2 expression were compared to control shRNA or GFP, respectively using Student *t*-test. *: $P<0.05$, **: $P<0.01$ and ***: $P<0.001$. Larger images of immunoblots are shown in Supplementary Figure S13b.

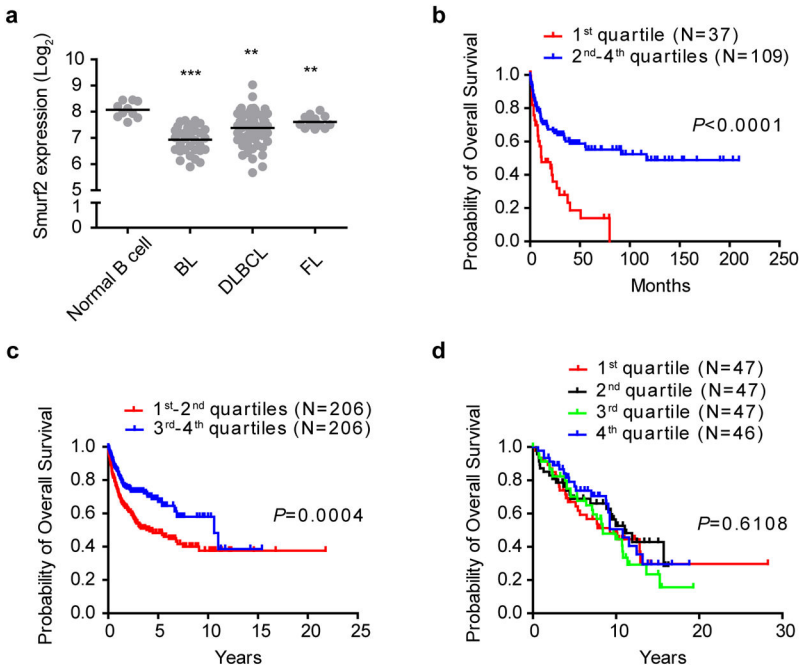

Figure 9. The level of Smurf2 expression correlates with overall survival of human DLBCL patients

(**a**) Dot plot of Smurf2 expression in normal B cells (N=10), Burkitt's lymphoma (BL, N=33), DLBCL (N=60) and follicular lymphoma (FL, N=14). One-way ANOVA is used to compare tumors with normal B cells. **: $P<0.01$ and ***: $P<0.001$. Kaplan-Meier curves of overall survival of patients in human B-cell lymphoma datasets (**b**) GSE4475, (**c**) GSE10846 and (**d**) a follicular lymphoma dataset plotted according to the level of Smurf2 expression, with the 1st quartile having the lowest Smurf2 expression. The log-rank test is used for statistical analysis.

Table 1

Univariate and multivariate analyses of prognostic factors associated with DLBCL patient overall survival

	Univariate analysis		Multivariate analysis	
Variables	**HR (95% CI)[a]**	***P***	**HR (95% CI)[a]**	***P***
GSE4475 (N=102)[b]				
Age[c]	2.35 (1.41–3.92)	0.001	1.94 (0.97–3.90)	0.062
Ann Arbor stag [d]	2.16 (1.28–3.65)	0.004	2.60 (1.37–4.94)	0.004
Ki-67 score[e]	0.97 (0.55–1.72)	0.912	1.26 (0.62–2.56)	0.526
Myc translocation[f]	1.11 (0.68–1.81)	0.68	1.38 (0.68–2.80)	0.379
Subtype[g]	2.26 (1.34–3.82)	0.002	2.12 (1.10–4.07)	0.025
Smurf2 expression[h]	2.68 (1.64–4.39)	<0.001	2.48 (1.24–4.93)	0.01
GSE10846 (N=311)[b]				
Age[c]	2.05 (1.47–2.86)	<0.001	1.41 (0.94–2.11)	0.099
Ann Arbor stage[d]	1.82 (1.31–2.52)	<0.001	0.95 (0.61–1.47)	0.805
Subtype[g]	2.81 (1.98–3.99)	<0.001	2.17 (1.49–3.16)	<0.001
Revised IPI score[i]	3.20 (2.31–4.42)	<0.001	2.90 (1.84–4.58)	<0.001
Smurf2 expression[j]	1.72 (1.28–2.42)	<0.001	1.51 (1.05–2.18)	0.027

[a] HR: hazard ration; CI: confidence interval;

[b] Only patients with complete information in all variables were used;

[c] Age: ≥60 vs. <60 years;

[d] Ann Arbor stage: III and IV vs. I and II;

[e] Ki-67 score: ≥95% vs. <95%;

[f] Myc translocation: presence vs. absence;

[g] Subtype: ABC vs. GCB;

[h] Smurf2 expression: Q1 vs. Q2-Q4;

[i] Revised IPI score: high (3, 4 and 5) vs. intermediate (1 and 2) and low (0);

[j] Smurf2 expression: Q1+Q2 vs. Q3+Q4.